The Role of Nonadiabatic Coupling in Bond-Selective Dissociations: Two-Dimensional Model Calculations

Toshiyuki Takayanagi* and Atsushi Yokoyama

Advanced Science Research Center, Japan Atomic Energy Research Institute, Tokai-mura, Naka-gun, Ibaraki 319-11

(Received March 9, 1995)

The photodissociation dynamics of the model CH_2XY (X and Y are halogen atoms) molecule was studied using a time-dependent quantum mechanical method in two dimensions. Simple functional forms were employed as two diabatic potential energy surfaces which correspond to the excited states of C–X (n–σ^*) and C–Y (n–σ^*). Bond selectivity in the photodissociation is quantitatively examined in terms of the coupling strength between the two surfaces. A method to predict the bond selectivity in the photodissociations is also discussed on the basis of the results of *ab initio* molecular orbital calculations.

Artificial control of reaction channels in unimolecular photodissociations is a challenging problem in the field of physical chemistry. The unimolecular dissociation of isolated molecules following infrared multiphoton excitation in the ground electronic state can successfully be understood by statistical theories; i.e., dissociation of the weakest chemical bond in the molecule occurs.[1] In other words, the rapid intramolecular vibrational energy redistribution inhibits the bond selectivity. Recently, bond selective dissociations have been observed in several experimental studies using excitation to the excited electronic states.

Butler et al.[2] have reported the selective dissociation of a C–Br bond over a weaker C–I bond following excitation of CH_2BrI at 210 nm, which corresponds to an n–σ^* transition of the C–Br bond. On the other hand, both C–Br and C–I bond dissociations were observed at 248 nm, the absorption peak due to C–I (n–σ^*). Butler's group has also reported that bond-selective dissociation is observed for CH_3SH,[3] $BrCH_2COCl$,[4,5] and $BrCH_2CH_2COCl$,[6] although the excitation processes are slightly different from the case of CH_2BrI. Another bond-selective dissociation has been found in the photodissociation of monodeuterated water using various excitation procedures.[7,8] Very recently, the photodissociation dynamics of $CBrF_2CHClF$ following electronic excitation at both 157 and 193 nm has been investigated in our laboratory.[9] It was found that preferential C–Cl bond dissociation over the weaker C–Br bond occurs when the molecule is excited at 157 nm corresponding to the C–Cl (n–σ^*) transition, while only C–Br bond dissociation is observed when the molecule is excited at 193 nm.

Das and Tannor[10] theoretically studied the photodissociation dynamics of $CBrF_2ClF_2$, for which bond-selective dissociations have not been observed,[11,12] by using a time-dependent wave packet method. They employed simple analytical functions for the C–Br (n–σ^*) and C–I (n–σ^*) diabatic potential energy surfaces and a coupling between the surfaces. Potential parameters were determined so as to reproduce the experimental absorption spectrum and the experimental branching ratio of I to Br. They have applied the same model to the CH_2BrI system; however, they concluded that the experimental results by Butler et al.[2] could not be explained by the same coupling. Thus they have suggested that the electronic coupling between the excited electronic states of C–Br (n–σ^*) and C–I (n–σ^*) for CH_2BrI is somewhat smaller than that for $CBrF_2ClF_2$.

Motivated by the above studies, we have theoretically investigated the dissociation dynamics of dihalogenated molecules in order to elucidate the main factors determining the bond selectivity in photodissociation. As a prototype molecule, CH_2XY (X and Y are halogen atoms) was chosen. The dynamics of dissociation was treated in two dimensions. Two diabatic potential energy surfaces corresponding to the C–X (n–σ^*) and C–Y (n–σ^*) excited states were used and a simple analytical function was employed as a coupling element between the two diabatic surfaces. The strength of the coupling element was then systematically changed. The purpose of the present study is to clarify quantitatively the relation between the strength of the coupling element and the bond selectivity in the photodissociation of dihalogenated molecules. In addition, a method to predict the bond selectivity from the results of *ab initio* electronic structure calculations is discussed.

Procedure of Dynamical Calculations and Construction of Potential Energy Surfaces

In order to treat the dissociation dynamics quantitatively, we have carried out time-dependent wave packet calculations[13] using simple model potentials in the diabatic representation. The time-dependent Schrödinger equations to be solved are given by ($\hbar$=1)

$$i\frac{\partial}{\partial t}\phi_1 = (T+V_{11})\phi_1 + V_{12}\phi_2,$$
$$i\frac{\partial}{\partial t}\phi_2 = (T+V_{22})\phi_2 + V_{12}\phi_1, \quad (1)$$

where T is the kinetic energy operator, V_{11} and V_{22} are the diabatic potential energy surfaces, V_{12} is the coupling element, and ϕ_1 and ϕ_2 are the time-dependent wave functions. We here treat the molecule CH_2XY as a pseudotriatomic molecule, where the first atom is X, and the second is Y, and the third is CH_2. The two-dimensional kinetic energy operator T is given by

$$T = -\frac{\partial^2}{2\mu_{11}\partial {r_1}^2} - \frac{\partial^2}{2\mu_{22}\partial {r_2}^2} - \frac{\cos\theta\partial^2}{\mu_{12}\partial r_1\partial r_2}, \quad (2)$$

where r_1 is the distance between X and C, r_2 is the distance between Y and C, and the reduced masses are denoted by

$$\mu_{11} = m_X m_{CH_2}/(m_X + m_{CH_2}),$$
$$\mu_{22} = m_Y m_{CH_2}/(m_Y + m_{CH_2}),$$
$$\mu_{12} = m_{CH_2}. \quad (3)$$

In the actual calculations, we choose Cl as X and Br as Y. θ is the X–C–Y equilibrium angle in the ground electronic state and is set to be 113°, which was determined from *ab initio* molecular orbital calculations of CH_2BrCl at the MP2/LANL1DZ level of theory using a GAUSSIAN92[16] package program. V_{11} and V_{22} are the diabatic potential energy surfaces for the excited states of C–X (n–σ^*) and C–Y (n–σ^*), respectively. These potentials can be expressed as the sum of an exponential function and a Morse function as follows:[10,14]

$$V_{11}(r_1,r_2)=V_1 e^{-\alpha_1(r_1-r_{e1})}+D_{e2}(1-e^{-\beta_2(r_2-r_{e2})})^2+E_1, \quad (4)$$

and

$$V_{22}(r_1,r_2)=V_2 e^{-\alpha_2(r_2-r_{e2})}+D_{e1}(1-e^{-\beta_1(r_1-r_{e1})})^2+E_2. \quad (5)$$

The Morse parameters for the C–Cl and C–Br bonds are taken from the vibrational frequencies and the geometry of CH_2BrCl in the ground-state. The potential parameters are taken as V_1=3.10 eV, V_2=3.51 eV, α_1=α_2=1.89 Å^{-1}, r_{e1}=1.75 Å, r_{e2}=1.96 Å, β_1=β_2=1.89 Å^{-1}, D_{e1}=3.60 eV, D_{e2}=3.0 eV, E_1=3.60 eV, and E_2=3.0 eV. The coupling element V_{12} between the two diabatic potentials is given by

$$V_{12} = A/(1+e^{\gamma_1(r_1-r_{e1})+\gamma_2(r_2-r_{e2})}). \quad (6)$$

The same function was used in the studies of photodissociations for $CBrF_2ClF_2$[10] and CH_2I_2.[14] The parameter A mainly determines the overall strength of the coupling element and is systematically changed in the present calculations. The other parameters are taken as γ_1=γ_2=0.5 Å^{-1}.

For the ground state potential, we employ the sum of two Morse potentials as follows:

$$V_g(r_1,r_2)=D_{e1}(1-e^{-\beta_1(r_1-r_{e1})})^2+D_{e2}(1-e^{-\beta_2(r_2-r_{e2})})^2. \quad (7)$$

The Morse parameters used are the same as those for the excited states. The wave function for the ground state is calculated using a basis set expansion method, where the standard harmonic oscillator basis is used in each coordinate. The initial wave packets are prepared as[13]

$$\phi_1(t=0) = \mu_{1g}\chi,$$
$$\phi_2(t=0) = \mu_{2g}\chi, \quad (8)$$

where μ_{1g} and μ_{2g} are the transition dipole moments to the excited states of C–Cl (n–σ^*) and C–Br (n–σ^*), respectively, and χ is the ground-state wave function. The ground vibrational state is used for χ. In the present calculations, the two transition dipole moments are assumed to be the same constants for simplicity. In addition, we consider the transitions to the two electronic excited states in the A' symmetry because the potential surfaces of the excited states in the A'' symmetry have essentially the same characteristics as the A' surfaces. This is the reason why we employ two potential surfaces for the excited states.

In order to propagate ϕ_1 and ϕ_2 in time, the method of Tal-Ezer and Kosloff,[15] in which the time-evolving wave packet is expanded in the Chebychev polynomials, was used. The fast Fourier transform method was adopted to evaluate the action of the kinetic energy operator on the wave function. Grid points of (256×256) spanning from 1.0 to 6.0 Å in each coordinate were employed in each wave packet. The total absorption cross sections were calculated directly from the autocorrelation function. The partial cross sections were obtained using a standard projection method of the total wave function on the eigenfunctions of asymptotic wave functions in each coordinate. The details of the method are described in Ref. 13. The method of Das and Tannor[10] was also employed in order to check the accuracy of our numerical calculations of the partial cross sections.

Results and Discussion

A. Results of Dynamical Calculations. Figure 1 shows the total absorption cross sections and the dissociation cross sections for the CH_2Br+Cl and CH_2Cl+Br channels as a function of the excitation energy for various coupling parameters A. When parameter A is 0.1 eV, the dissociation cross sections for the Cl and Br product channels have a single peak. The

cross section for the Cl product channel shows a peak at around 7.2 eV corresponding to the C–Cl (n–σ^*) excitation. On the other hand, the cross section for the Br product channel shows a peak at around 6.2 eV corresponding to the C–Br (n–σ^*) excitation with a small tail in the blue region. As potential parameter A becomes larger, the cross section for the Br product channel has one more peak at an excitation energy of 7.2 eV. In addition, the height of the peak becomes larger as the coupling parameter becomes larger. On the contrary, although the peak height is slightly changed, the cross section for the Cl product channel has a single peak. Figure 2 shows the excitation energy dependence of the probability of producing the Cl product channel. Even

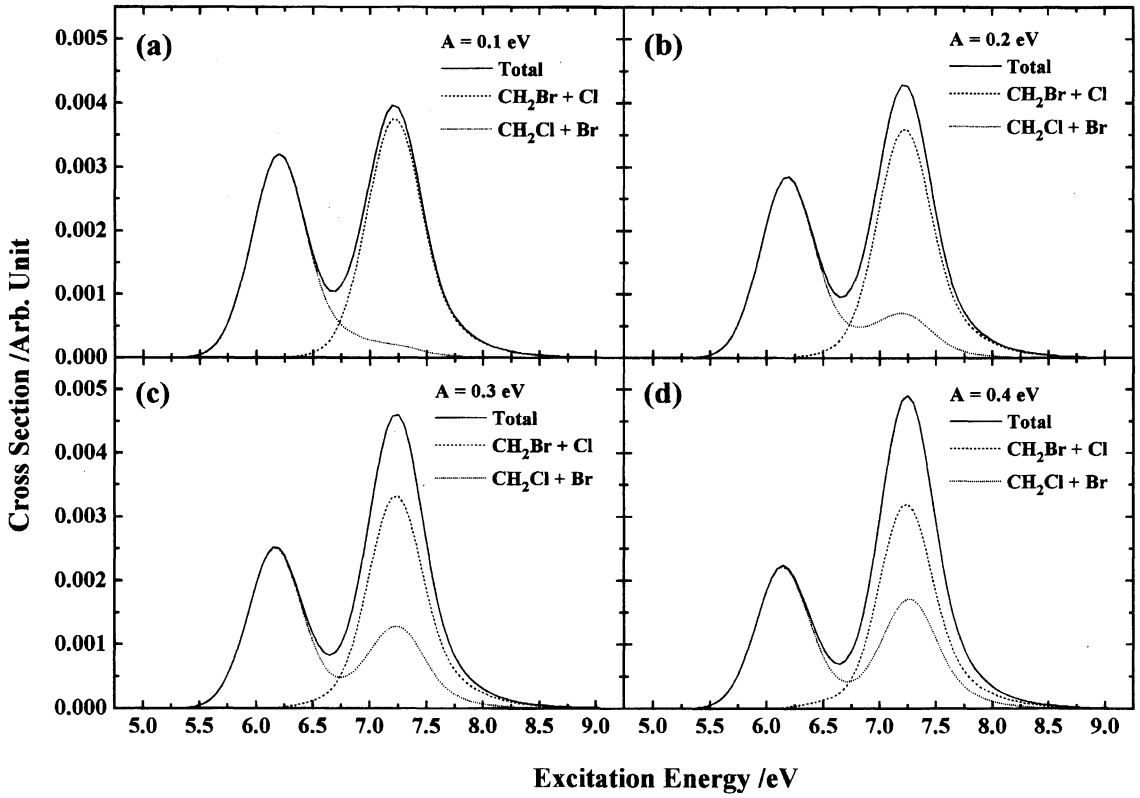

Fig. 1. Excitation energy dependence of total absorption cross section and cross sections for the Cl and Br product channels with various potential parameters A. (a) A=0.1 eV, (b) A=0.2 eV, (c) A=0.3 eV, (d) A=0.4 eV.

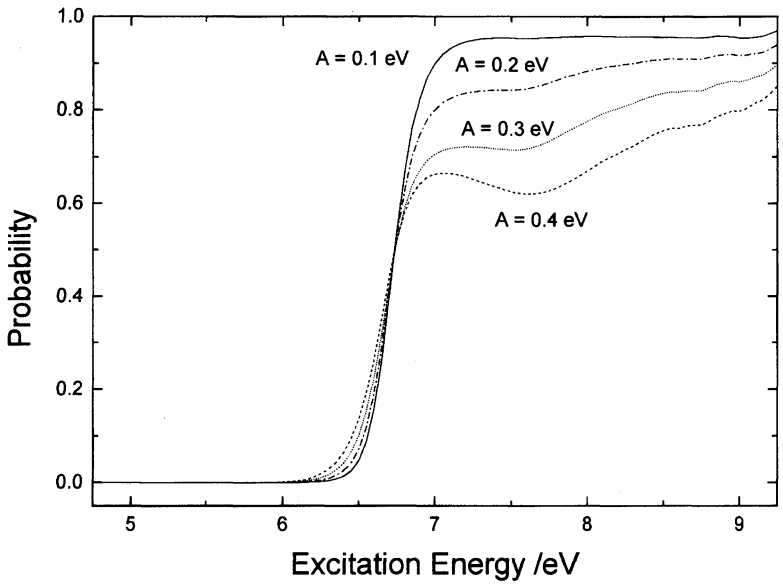

Fig. 2. Excitation energy dependence of the probability for producing the CH_2Br+Cl channel.

if coupling parameter A is 0.1 eV, the maximum probability for the Cl product channel is about 96%. As the excitation energy becomes larger, the probability for the Cl product channel becomes larger. However, the magnitude of the absorption cross section is, of course, quite small. Thus, Figs. 1 and 2 indicate that coupling parameter A should be small enough in order to make the bone-selective dissociation possible.

For understanding the dynamics of the CH_2BrCl photodissociation more precisely, we present the time propagation of the wave packets on the two potential energy surfaces in Figs. 3 and 4 in the diabatic representation. The coupling parameter (A) employed is 0.3 eV. The wave packet on the C–Cl (n–σ^*) surface is separated into two parts at t=400 au (1 au in time=2.4×10^{-17} s) One part moves toward the crossing region and disappears from the C–Cl (n–σ^*) surface at a larger propagation time. But the other part of the wave packet on the C–Cl (n–σ^*) surface moves directly toward the Cl product channel. This wave packet corresponds to the direct dissociation of the C–Cl bond. On the other hand, the wave packet on the C–Br (n–σ^*) surface is somewhat complicated. At longer times, t>400 au, the wave packet has two parts; one corresponds to the direct dissociation of the C–Br bond, while the other part comes from the C–Cl (n–σ^*) surface through the crossing seam. It is also noted that the wave packet having come from the C–Cl (n–σ^*) surface shows vibrationally

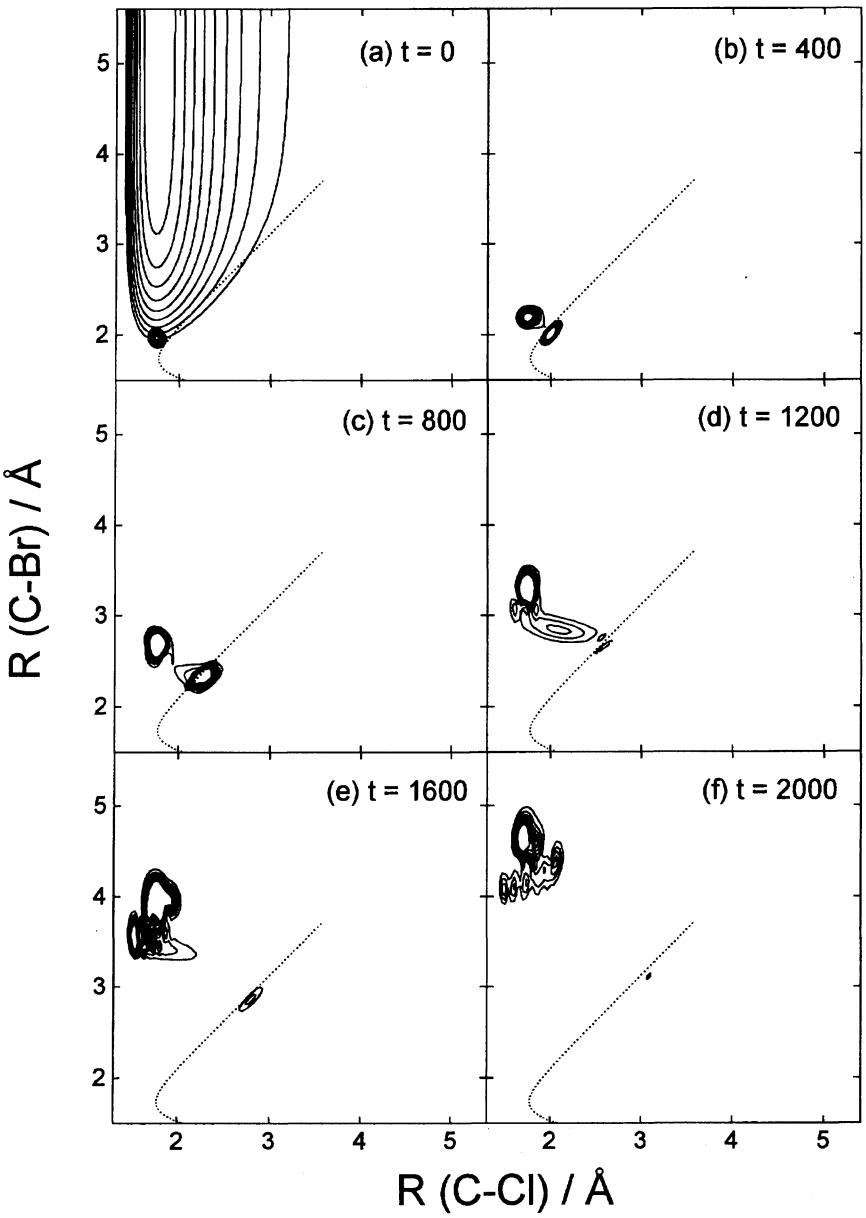

Fig. 3. Moving wave packet on the C–Br (n–σ^*) potential energy surface. The wave packets are drawn in the diabatic representation. Time is in atomic unit (1 au=2.4×10^{-17} s). Contours are drawn for the C–Br (n–σ^*) potentials. Dotted lines indicate the crossing seam.

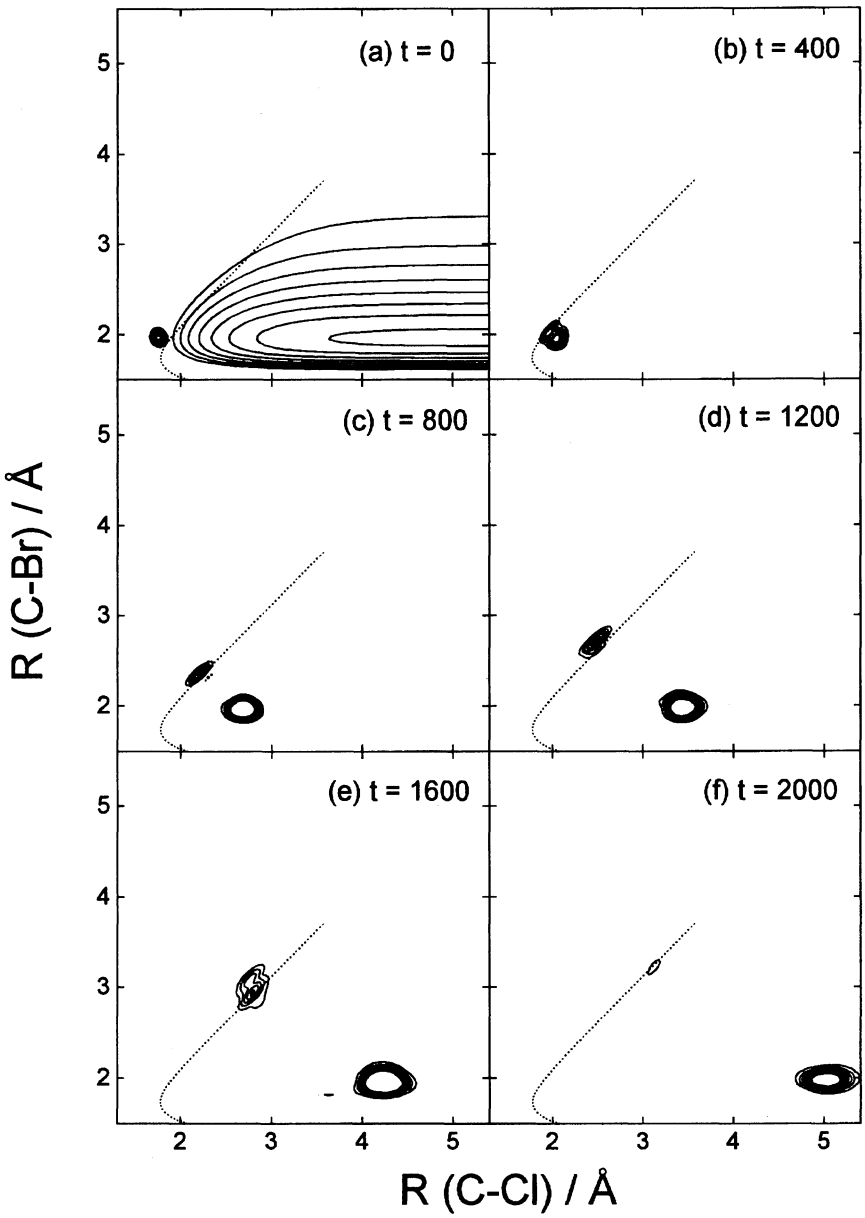

Fig. 4. Moving wave packet on the C–Cl (n–σ^*) potential energy surface. The wave packets are drawn in the diabatic representation. Time is in atomic unit. Contours are drawn for the C–Cl (n–σ^*) potentials. Dotted lines indicate the crossing seam.

excited behavior in the C–Cl coordinate. Thus, this wave packet's dynamics is reflected in the excitation energy dependence of the cross sections for the Cl and Br product channel as shown in Fig. 1. The additional peak in the cross section for the Br product channel corresponds to the nonadiabatic transition from the C–Cl (n–σ^*) surface to the C–Br (n–σ^*) surface.

The wave packet dynamics described above is easily explained from the crossing behavior between the two potential energy surfaces. The wave packet on the C–Br (n–σ^*) potential does not encounter the crossing seam because the initial wave packet exists in the region of the CH_2Cl+Br product channel. On the other hand, the wave packet on the C–Cl (n–σ^*) surface encounters the crossing seam when the wave packet moves toward the region of the CH_2Br+Cl channel.

B. Prediction of the Bond Selectivity in the Photodissociation from *ab initio* Molecular Orbital Calculations. In the previous section, we employed simple functional forms as the diabatic potential energy surfaces in order to calculate the dynamics of photodissociation for the model molecule CH_2XY. In principle, we are able to compute the global potential energy surfaces including excited states by using a modern *ab initio* molecular orbital method. However, such a calculation is a time-consuming procedure because the derivatives of the electronic wave functions with respect to the nuclear coordinates are also needed for the quantitative treatment of the multisurface problems. The calculations of the derivatives are not available in gen-

eral *ab initio* computational programs. Therefore, in this section we shall consider a simple method to predict the bond selectivity in the photodissociation in terms of the magnitude of the separation at the avoided crossing region of the two excited-state potentials.

Figure 5 shows the schematic potentials along the C–Cl coordinate for the photodissociation of CH_2BrCl. Solid lines represent the diabatic potentials V_{11} and V_{22}. Dotted lines represent adiabatic potentials V_a and V_b. These potentials are given as

$$V_a = \frac{1}{2}\left\{V_1 + V_2 + \sqrt{(V_1 - V_2)^2 + 4V_{12}^2}\right\}, \quad (9)$$

$$V_b = \frac{1}{2}\left\{V_1 + V_2 - \sqrt{(V_1 - V_2)^2 + 4V_{12}^2}\right\}. \quad (10)$$

The minimum separation between V_a and V_b is denoted as S_{12}. Table 1 summarizes the minimum separations calculated from the model potentials employed in the previous dynamical calculations. The minimum separation S_{12} is approximately proportional to the coupling parameter A defined in Eq. 6. The dynamical results obtained in the previous section indicate that the bond selectivity in the photodissociation may be attained with a relatively small value of S_{12}, which is typically less than 0.2 eV.

On the other hand, we can easily calculate the adiabatic potentials by using an *ab initio* molecular orbital theory. As a trial, we calculated the potential energy surfaces of the excited states for both CH_2BrCl and $CBrF_2CHClF$ using the GAUSSIAN92 program.[16] The ground state was calculated at the MP2 level of theory with an effective core potential basis set of LANL1DZ.[16] The internal coordinates other than those of C–Cl and C–Br were optimized at the same level of theory. The excitation energies were calculated using the configuration interaction with single excitations (CIS) method. The adiabatic potential energy surfaces obtained for CH_2BrCl are presented in Fig. 6. Figure 6(a) shows the repulsive potential which corresponds to V_b, while Fig. 6(b) shows the bound-like potential corresponding to V_a. From the potential surfaces in Fig. 6, we can estimate the minimum separation S_{12} between these two surfaces. Table 2 summarizes the minimum separation obtained for both CH_2BrCl and $CBrF_2CHClF$. It is found that the minimum separation for CH_2BrCl is about three times as large as that for $CBrF_2CHClF$. Although the excited-state surfaces shown in Fig. 6 are for singlet states, essentially the same results are obtained for triplet states.

From the dynamical results obtained in the previous section and the present *ab initio* calculations, it may be concluded qualitatively that bond-selective dissociation would not be observed for CH_2BrCl. On the other hand, the bond-selective dissociation observed experimentally for $CBrF_2CHClF$[9] can be explained by the small coupling strength between the C–Cl (n–σ^*) and C–Br (n–σ^*) potentials. Such a small coupling may come from the spatial separation between the C–Cl and C–Br bonds. Of course, our conclusion may be valid only when the transition between singlet and triplet states can be ignored. In order to obtain more quantitative conclusions, the spin-orbit interaction should be considered. Nevertheless, we believe that our simple model gives a qualitative picture for understanding the

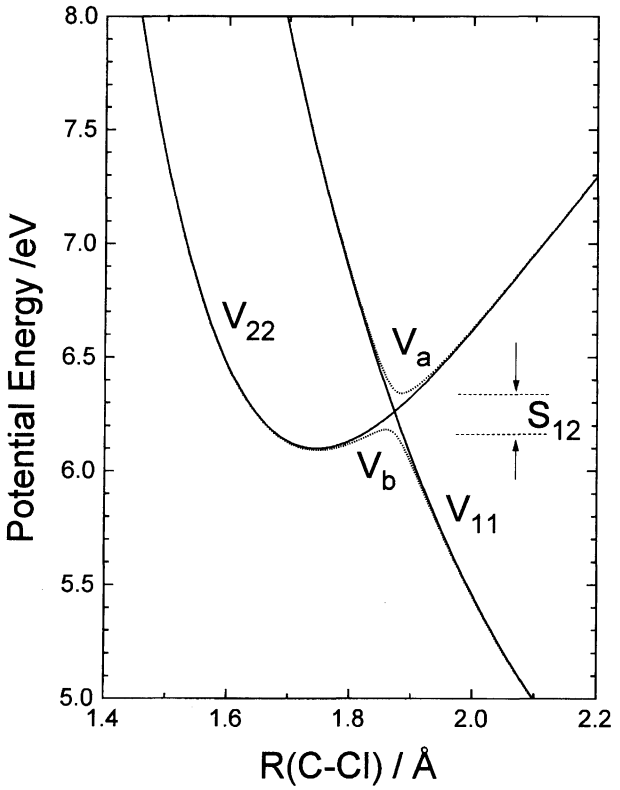

Fig. 5. Schematic potential energies along the C–Cl coordinate for model CH_2XY molecule. V_{11} and V_{22} are diabatic potentials, while V_a and V_b are adiabatic potentials. S_{12} is the minimum separation between two adiabatic potentials.

Table 1. Relation between the Potential Parameter A and the Minimum Separation S_{12}

A/eV	S_{12}/eV
0.1	0.115
0.2	0.238
0.3	0.346
0.4	0.488

The distance between C and Br is assumed to be the equilibrium distance in the ground-state.

Table 2. The Minimum Separation S_{12} Obtained from *ab initio* CIS Calculations for CH_2BrCl and $CBrF_2CHClF$

Molecule	S_{12}/eV
CH_2BrCl	0.332
$CBrF_2CHClF$	0.100

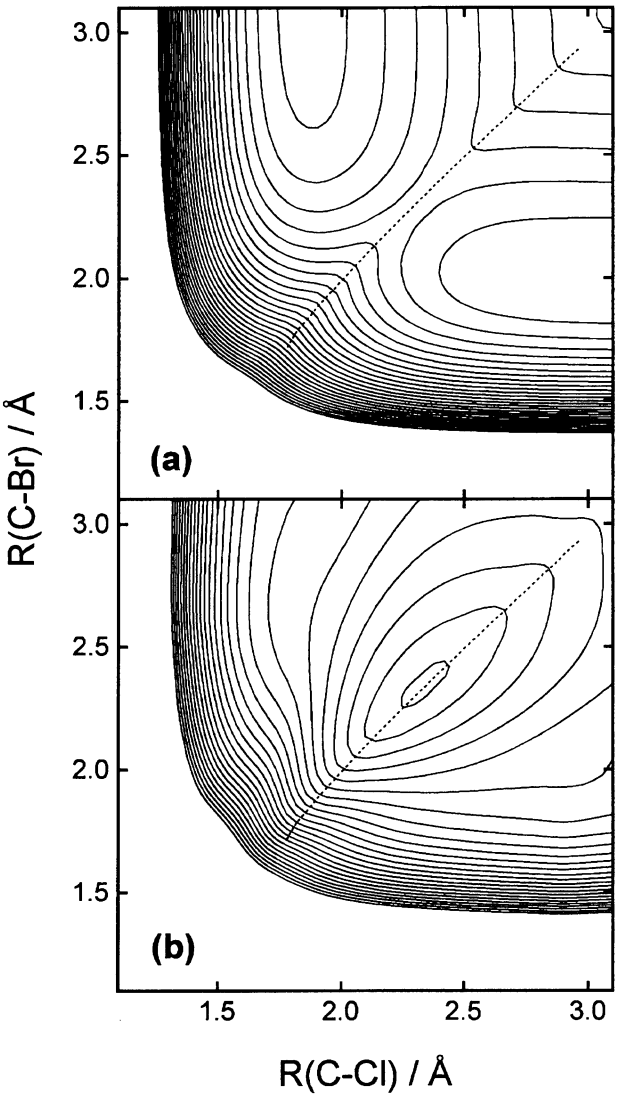

Fig. 6. Contour plots of the two adiabatic potential energy surfaces obtained by *ab initio* molecular orbital calculations at the CIS/**LANL1DZ** level of theory. (a) is for the first excited state, and (b) is for the second excited state. Dashed lines indicate the crossing seam.

bond selectivity in the photodissociation.

Conclusion and Future Work

We have demonstrated that nonadiabatic coupling elements play an important role in the bond selectivity in the photodissociation of a dihalogenated molecule. It was found that the small coupling strength between the two excited states is needed for bond selectivity. We have also presented the potential energy surfaces obtained by simple *ab initio* molecular orbital calculations. The *ab initio* CIS calculations give a relatively large coupling in the excited states of CH_2BrCl, while a smaller coupling is obtained for $CBrF_2CHClF$. This suggests that the bond-selective dissociations would not be observed for CH_2BrCl. However, the accuracy of the *ab initio* method is strongly dependent on the basis functions as well as the electron correlation effects included in the level of the theory. It is well-known that the CIS method does not include electron correlation effects. In addition, we have completely ignored the spin-orbit interactions. Thus, in order to obtain more accurate potential surfaces, a more accurate theory for electronic structure calculations such as a multireference configuration interaction (MRCI) theory is probably necessary. However, this is limited to simple molecules containing a small number of electrons even if a modern supercomputer is available.

We may conclude tentatively that the difference in the coupling strength between CH_2BrCl and $CBrF_2CHClF$ is attributed to the spatial separation of the C–Cl and C–Br bonds. However, the same conclusion could not be drawn from the experimental results on the photodissociations of CH_2BrI and $CBrF_2ClF_2$. As already stated in the Introduction, bond-selective dissociation occurs for CH_2BrI but does not occur for $CBrF_2ClF_2$, although the spatial separation between the C–Br and C–I bonds for $CBrF_2ClF_2$ is larger than that for CH_2BrI. In order to explain the above experimental results, potential energy surface calculations by the *ab initio* molecular orbital theory are needed. In addition, a spin-orbit interaction should be included since the spin-orbit coupling for the I atom is much larger than that for the Cl atom.

It is encouraging that the bond selectivity in the photodissociation of the dihalogenated molecule is simply predicted by the coupling strength between the two excited n–σ^* potentials. For example, in the case of an alkane molecule like X–$(CH_2)_n$–Y, one may expect that the coupling between the two excited states of C–X (n–σ^*) and C–Y (n–σ^*) becomes smaller because the X and Y atoms are spatially separated. These experiments as well as the theoretical calculations for such a molecule are currently underway in our laboratory.

References

1) P. A. Schulz, Aa. S. Sudbø, D. J. Krajnovich, H. S. Kwok, T. R. Shen, and Y. T. Lee, *Ann. Rev. Phys. Chem.*, **30**, 379 (1979).

2) L. J. Butler, E. J. Hintsa, S. F. Shane, and Y. T. Lee, *J. Chem. Phys.*, **86**, 2051 (1987).

3) J. S. Keller, P. W. Kash, E. Jensen, and L. J. Butler, *J. Chem. Phys.*, **96**, 4324 (1992).

4) M. D. Person, P. W. Kash, S. A. Schfield, and L. J. Butler, *J. Chem. Phys.*, **95**, 3843 (1991).

5) M. D. Person, P. W. Kash, and L. J. Butler, *J. Chem. Phys.*, **97**, 355 (1992).

6) P. W. Kash, G. C. G. Waschewsky, L. J. Butler, and M. M. Francl, *J. Chem. Phys.*, **99**, 4479 (1993).

7) N. Shafer, S. Satyapal, and R. Bersohn, *J. Chem. Phys.*, **90**, 6807 (1989).

8) R. L. Vander Wal, J. L. Scott, and F. F. Crim, *J. Chem. Phys.*, **92**, 803 (1990).

9) A. Yokoyama, T. Takayanagi, and G. Fujisawa, *J.*

Chem. Phys., in press.
10) S. Das and D. Tannor, *J. Chem. Phys.*, **91**, 2324 (1989).
11) D. Krajnovich, L. J. Butler, and Y. T. Lee, *J. Chem. Phys.*, **81**, 3031 (1984).
12) C. A. Wight and S. R. Leone, *J. Phys. Chem.*, **87**, 5299 (1983).
13) R. Schinke, "Photodissociation Dynamics," Cambridge University, New York (1993).
14) J. Zhang, E. J. Heller, D. Huber, D. G. Imre, and D. Tannor, *J. Chem. Phys.*, **89**, 3602 (1988).
15) Tal-Ezer and Kosloff, *J. Chem. Phys.*, **81**, 3967 (1984).
16) "GAUSSIAN 92, Revision C.4," M. J. Frisch, G. W. Trucks, M. Head-Gordon, P. M. W. Gill, M. W. Wong, J. B. Foresman, B. G. Johnson, H. B. Schlegel, M. A. Robb, E. S. Replogle, R. Gomperts, J. L. Andres, K. Raghavachari, J. S. Binkley, C. Gonzalez, R. L. Martin, D. J. Fox, D. J. Defrees, J. Baker, J. J. P. Stewart, and J. A. Pople, Gaussian Inc., Pittsburgh, PA (1992).